Int. J. Nav. Archit. Ocean Eng. (2015) 7:490~499
http://dx.doi.org/10.1515/ijnaoe-2015-0035
pISSN: 2092-6782, eISSN: 2092-6790

A study on measurements of local ice pressure for ice breaking research vessel "ARAON" at the Amundsen Sea

Yong-Hyeon Kwon[1], Tak-Kee Lee[2] and Kyungsik Choi[3]

[1]*Department of Ocean System Eng., Graduate School, Gyeongsang National University, Tongyeong, Korea*
[2]*Department of Naval Archi. & Ocean Eng., Gyeongsang National University, Institute of Marine Industry, Tongyeong, Korea*
[3]*Department of Ocean Eng., Korea Maritime and Ocean University, Busan, Korea*

Received 17 July 2014; Revised 10 February 2015; Accepted 15 March 2015

ABSTRACT: *In this study, a local ice pressure prediction has been conducted by using measured data from two ice breaking tests that was conducted for a relatively big ice floe at Amundsen Sea in the Antarctica from January 31 to March 30 2012. The symmetry of load was considered by attaching strain gauges on the same sites inside the shell plating of ship at the port and the starboard sides in the bow thrust room. Using measured strain data, after the ice pressure was converted by the influence coefficient method and the direct method, the two values were found to be similar.*

KEY WORDS: Local ice pressure; Big floe; Amundsen sea; Influence coefficient method; Direct method.

INTRODUCTION

Due to melting of a large amount of ice in the Arctic Ocean mainly after the global climate change, many parts of the Northern Sea Routes have opened in recent years, and this created great interests on this region. It can be expected that these openings in the Northern Sea Route would further lead to a steady growth in trade, which in turn would place a demand for icebreakers and ice-strengthened ships. Thus, manufacture and development of these ice vessels are likely to rise faster, although several important factors related to the manufacture needs consideration in the first place. One important issue, in this regard, is when a ship comes in contact or collides with the ice in Arctic regions. It involves one of the ice loads and has significant impact on the structure of the ship.

The ice load can be divided into local ice load and global ice load for convenience (ABS, 2011). Local ice load is defined as the ice pressure that acts locally on some areas of plate and supporting materials, which compose the ship structure. The local ice pressure is also defined in all ice class regulations, and generally, this local ice pressure has been known to be dependent on the ice type, the ice thickness, the ice-ship interaction and the governing ice breaking mode (ISSC, 2012).

POLAR SEA of the US measured the local load at the Beaufort Sea in September and October, 1982 and Chukchi Sea in March and April, 1983. These are considered as the best available data among all that measured the local load using a strain gauge (St. John et al., 1990).

Corresponding author: *Tak-Kee Lee*, e-mail: *tklee@gnu.ac.kr*

The first measurement by Korean research teams was the one that was conducted in July and August, 2010 by using ARAON, the first Korean icebreaker (Kim et al., 2011). In this measurement, the research team selected an ice floe for the test and conducted measurements of ice thickness and other characteristics directly on that ice floe (Park et al., 2011; Kim et al., 2012). When the ice-ship interaction occurred, the effect of ship speed and ice thickness on the ice load was considered, and based on the measured values, a study on the method to convert the ice load into ice pressure was also conducted (Lee et al., 2013a; 2013b).

Researchers conducted measurements on ice load at Amundsen Sea from the end of January to the middle of March, 2012 (Kim et al., 2013). In this work, prior to the two ice breaking performance tests, characteristics of the ice were identified first. Using the measured values from the strain gauge at the bow, the ice pressure was calculated using both coefficient method and direct method. In the current study, the symmetry of stress applied on the ship has been also identified at the time of ice-ship contact and collision by attaching the strain gauges at the same position of port side and starboard side of the bow.

DATA MEASUREMENT AT AMUNDSEN SEA

Two ice breaking tests were carried out on Amundsen Sea of Antarctica in 2012. In these tests, for the purpose of measuring the local ice load acting on the bow and the side of the ship, the strain gauges were attached inside the shell plating of port and starboard side, between 106 frame and 111 frame of the lower part of second deck inside the bow thrust room, as shown in Fig. 1. The second deck was located at 7,100 A/B (7,100 *mm* above the baseline), and the design load waterline of ARAON was 6,800 A/B. The shell plate was made of EH36 grade steel and had a thickness of 34.5 *mm*. The reason why strain gauges were attached in this area is that this area was around the shoulder part of ARAON horizontally and was around the design waterline vertically. It is already known that local ice pressure is higher at the shoulder part than that in the other parts (St. John and Minnick, 1995).

The adopted strain gauges are a rectangular strain gauge rosette with a grid length of 5 *mm*, FRA-5-11-5LT (maker: Tokyo Sokki Kenkyujo). A strain gauge rosette with half-bridge connection of the above dimension is often used in engineering practice to find out strain states at specific points and MGCplus (maker: HBM) is used as the data acquisition system. Frame spacing is 800 *mm* and a dotted line in Fig. 1 means a stiffener with almost same dimension with the frame. As shown in Fig. 1, 21 strain gauge rosettes were attached. In the figure, L and R represent the port and the starboard side respectively. Gauges with numbers 1 to 10 were attached at the same position on both the sides, however, the R11 gauge was attached only to the starboard side as the port side was not a proper position to install.

The voyage route and the ice breaking test sites of ARAON vessel in the Amundsen Sea are shown as in Fig. 2 (Kim et al., 2013). The route covered the entire Amundsen Sea from Pine Island Glacier to Cape Burks, and the sites marked as SI 1 and SI 2 in the figure are the places where the ice breaking tests were conducted.

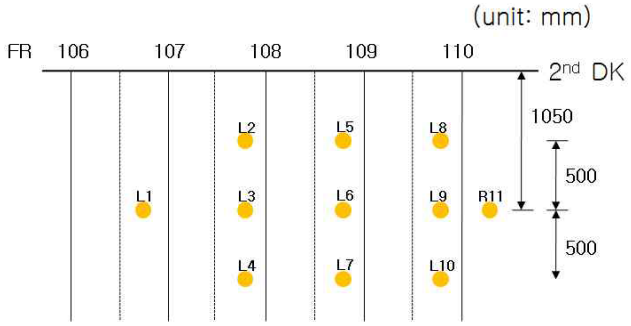

Fig. 1 Location of the strain gauges between Frame No. 106 and No. 111.

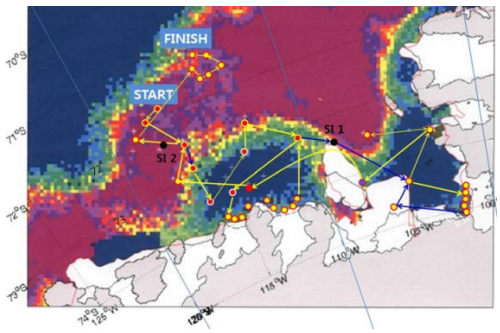

Fig. 2 Route of Araon and the Ice breaking test sites.

The ice floe of the first test had the size of about 900 *m* × 600 *m*, selected at the position of 73°30'43"S, 109°02' 11"W on February 21, 2012. Moreover, the ice floe was estimated to be one year old. The thickness of this ice floe is shown in Fig. 3, the horizontal axis shows the progress distance, and the vertical axis shows the thicknesses of the snow and the ice. The shape of ice was marked with a blue solid line, and the vertical distribution of the actual ice was expressed in the direction of the vertical axis.

The atmospheric temperature at the time of test was about -1℃, and the wind speed was about 12 *knot*. The draft at bow of ARAON was 7.04 *m*, and the center draft on the starboard side and the port side were 7.00 *m*, 7.04 *m* respectively.

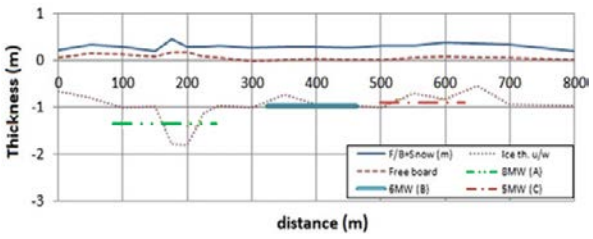

Fig. 3 Ice thickness and snow depth of the 1st ice floe.

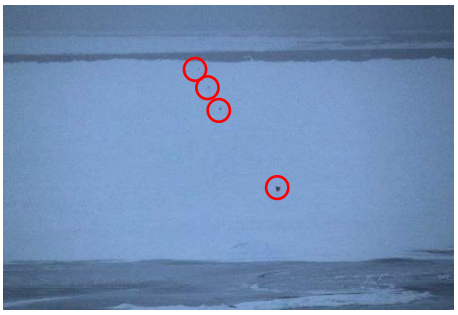

Fig. 4 Ice target for ice breaking in the Amundsen Sea (1st test).

Fig. 4 shows the pictures that were taken of the flag and the ice breaking path during the ice breaking test (Choi et al., 2012). The distances between the first and the second flag was 300 *m*, between the second and the third flag was 200 *m*, and between the third and the fourth flag was 300 *m*; therefore, the total distance measured was 800 *m*. Fig. 5 expresses the position of ARAON with GPS setting the coordinate points of latitude and longitude same as the real directions. It is shown that the south latitude became higher as it went down toward left, and the west longitude became lower as it went to the right. The test was conducted by changing the engine power as 8 *MW*, 6 *MW* and 5 *MW* for each section.

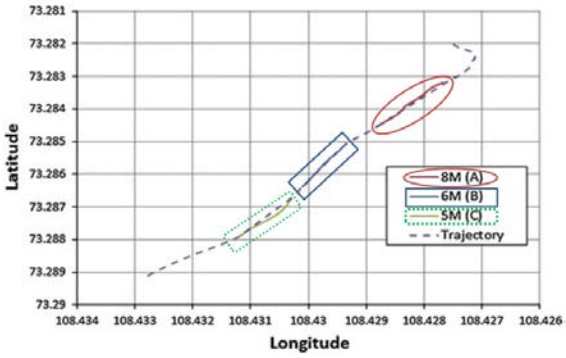

Fig. 5 Ship trajectory and power data from the 1st test.

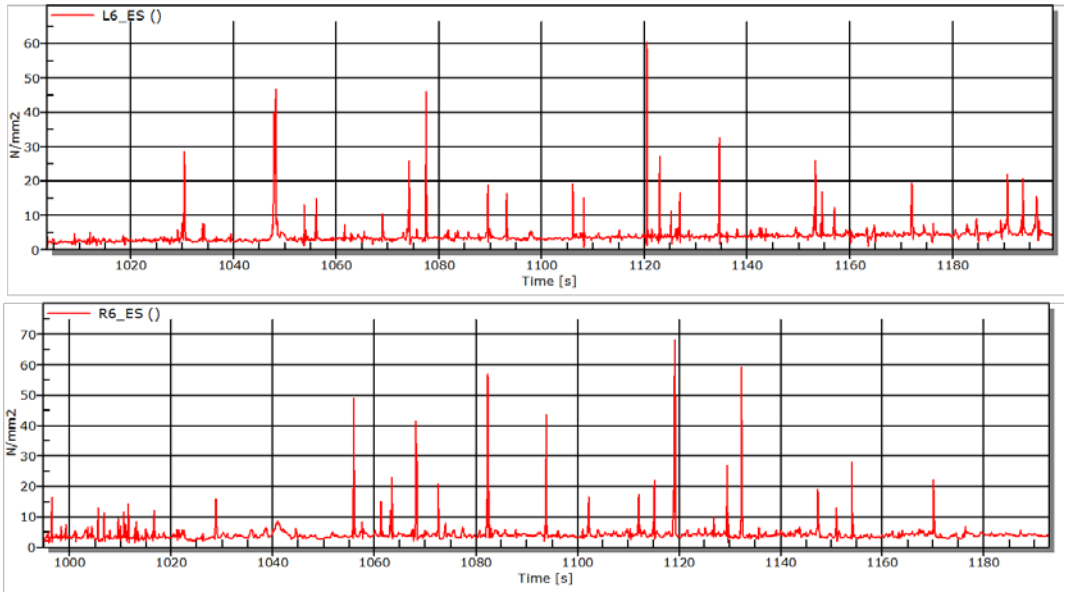

Fig. 6 Examples of data (equivalent stress) measured from strain no. L6 and R6 in the 1st test.

Fig. 6 shows the data measured from L6 and R6 strain gauges in the first test. The record duration of the first test was total 1,800 *second*, but an ice-induced strain was recorded just before 1,000 *second* to about 1,200 *second*. The record duration of the second test was about 4,430 *seconds*. The sampling rate was 50 *Hz*, and a Bessel lowpass filter with cut-off frequency of 5 *Hz* was adopted. To calculate the equivalent stress from the measured strain data by using Hooke's Law, the Young's modulus of the material used was 200 *GPa*.

The positions of the second test floe were 72°15'11"S, 117°49'32"W in March 04, 2012, and its size was about 1,100 *m* × 600 *m*, which had a structure with a little thick ridge at the center, as shown in Fig. 7. This floe was presumed to be of one year old which was relatively flat with one side blocked by a huge iceberg. The atmospheric temperature at the time of the test was about -4.5℃, and the wind speed was measured at about 12 *knots*. The draft at bow on the ship was 6.88*m*, the center draft on the starboard side was 6.71 *m* and that on port side was 6.84 *m*. Fig. 8 shows the test path of the second ice floe. In this test, the engine output was changed to 7 *MW* and 8 *MW*.

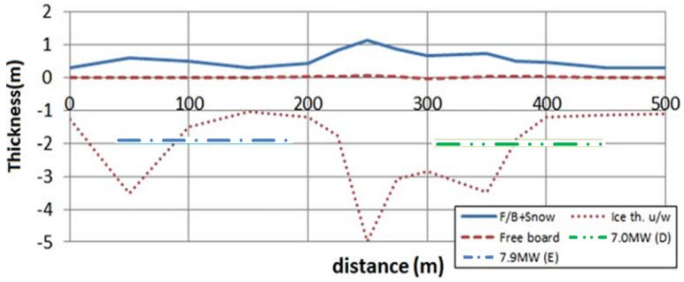

Fig. 7 Ice thickness and snow depth of the 2nd ice floe.

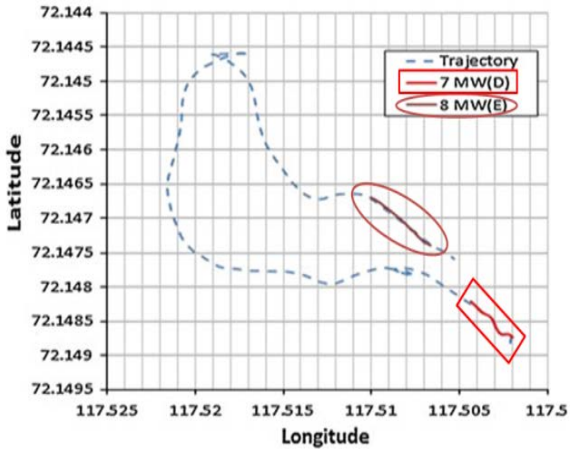

Fig. 8 Ship trajectory and power data from the 2nd test.

Table 1 Summary of the two big floes.

Ice floe No.		1	2
Location	Longitude	109°02'11"W	117°49'32"W
	Latitude	73°30'43"S	72°15'11"S
size	Length (*m*)	900	1,100
	Width (*m*)	600	600
Air temperature (℃)		-1	-4.5
Wind speed (*knots*)		12	12
Average compressive strength (*MPa*)		1.445	1.32
Average bending strength (*kPa*)		274	266

The summarized results for the ice floe characteristics from the first and second tests are shown in the Table 1. The average compressive strength for the first floe was 1.445 *MPa*, and the average bending strength was 274 *kPa*. The average compressive strength for the second floe was 1.32 *MPa* and the average bending strength 266 *kPa* (Ha et al., 2012). The compressive strength was measured directly from the ice core specimen using a simple on-site tester, and its bending strength was calculated from the experimental equation of Timco and O'Brien (1974).

CALCULATION OF THE LOCAL ICE PRESSURE

Among the ice breaking test data measured twice in the Antarctic Ocean, peak stress values higher than 20.0 *MPa* were selected to obtain the variation of the peak stress with the speed as shown in Fig. 9. In the second test, when the ship speed was about 3.42 *knot*, the peak stress of channel L10 at the port side was measured, to obtain the maximum value (180.7 *MPa*). The peak stress over 100 *MPa* was measured in the second test, and it is presumed that these are related to the existence of ice ridge in the middle of ice floe.

Theoretically, especially in case of global ice load the faster a ship's speed is, the greater the ice load that acts on the ship is. But the measured results are different as shown in Fig. 9. According to Kim et al. (2014), an ice load increases with a ship's speed up to a certain limit, after which it levels off (forms a plateau) or decreases, as shown in Fig. 8. This trend was also investigated by other researchers (St. John and Minnick, 1995; Tsoy et al., 1998). The reason for this particular trend is possibly because higher speed of a ship with a constant engine power can be achieved in thinner ice, which leads to lower ice load (Lee et al., 2013a).

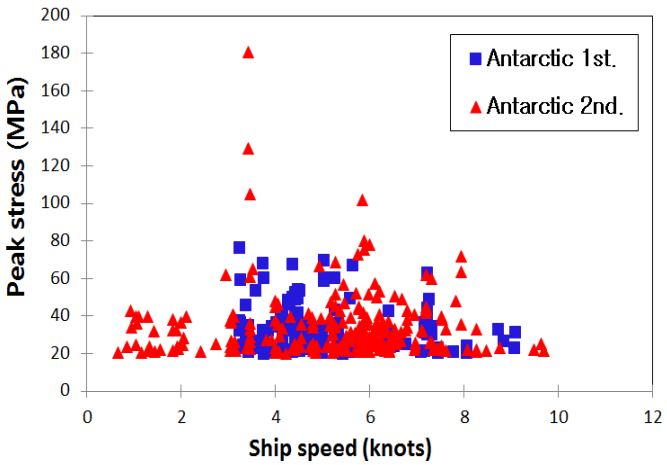

Fig. 9 Change in the peak stress with the ship's speed in the Amundsen Sea.

It is also mention-worthy that between the first and the second tests, in the former the ship followed the route exactly that had been pre-assigned to it, and the actual and intended ice breaking trajectory were similar (Fig. 5), However, in the second test, the pre-assigned straight course was not maintained all the time and some turns were made. This introduced some deviations from the intended ice breaking path (Fig. 8).

Influence coefficient method

When a value measured by the strain gauge is converted to the ice pressure, the influence coefficient method is used in general. In other words, when a pressure is applied on a specific part, the related strain develops not only at the pressure point but also in the vicinity area. Thus, to calculate the influence coefficient, pressure is applied to an area that is at the vicinity of and surrounds the actual target pressure point, with repeated calculations of the stress through structural analysis of the process (Lee et al., 2013b). Here, it is assumed that pressure with uniform distribution over a specific area is applied in normal direction against the side shell plating as selected by Ritch et al. (2008).

When the obtained influence coefficient was applied to the relation function of pressure vs stress, the following was obtained:

$$\{\sigma\} = [C]\{p\} \tag{1}$$

Here, $\{\sigma\}$, $\{p\}$ refer to stress and pressure vectors for each specified area respectively, and [C] refers to the influence coefficient matrix of pressure against stress (see Lee et al., 2013b, for details including matrix [C] of the ARAON).

CALCULATION OF ICE PRESSURE

The stress is an equivalent stress (generally, von-Mises stress), which can be calculated using the measured values from the three components of the rosette gauges. It was calculated using peak values obtained from the strain data measured from L3, L6 and L9 of port side and R3, R6 and R9 of starboard side in each of the two tests. If there is no data in neighboring area its stress value is assumed to be zero. For example, for the gauge L6, though measured values for two nearby vertical areas (that is, L5 and L7) were there, no data were available for other 6 areas, including the areas between L2 and L5, and L3 and L6. Furthermore, as the data from R6 gauge on the starboard side in the second test was not measured well, the calculation result of R6 was omitted.

In Tables 2~3, ICM is the calculated ice pressure value using the influence coefficient method, Direct is the calculated ice pressure value using the direct method. The direct method was to calculate the pressure directly by using only the relationship between pressure and stress for the considered area (that is, some area surrounding one strain gauge), regardless of the effect of pressure acting in the neighboring area (that is, the influence coefficient). ICM/D shows the ratio of the influence coefficient method to the direct method. The maximum ice pressure, calculated by the influence coefficient method from the second test at L9 on the port side was 2.836 *MPa*, whereas, the ice pressure calculated by the direct method was 2.632 *MPa*.

Fig. 10 and 11 show the graphs which compare the ratio of the influence coefficient method to the direct method of each port side and starboard side respectively with y=x line graph for the first and the second tests. Values used in the graphs are peak values over 20.0 *MPa* from both the tests. The difference between a slope of y=x graph, 1 and an average value of ICM/D, 1.0238 is as small as 0.0238, and the graph shows that almost all values are close to the y=x graph, indicating a very little difference between the direct and the influence coefficient methods. Therefore, it is practically possible to calculate the ice pressure even when the direct method is applied.

Table 2 Calculated ice pressures on the port side and the starboard side (1st test). (unit : *MPa*)

L3			L6			L9		
ICM	Direct	ICM/D	ICM	Direct	ICM/D	ICM	Direct	ICM/D
2.062	1.940	1.063	1.658	1.516	1.094	1.828	1.688	1.083
1.405	1.316	1.067	1.178	1.238	0.951	1.004	1.130	0.889
0.987	1.024	0.963	1.273	1.171	1.087	0.922	1.006	0.916
1.027	1.016	1.011	0.951	1.152	0.825	0.936	0.884	1.059
Port side average ICM/D = 1.003								
R3			R6			R9		
ICM	Direct	ICM/D	ICM	Direct	ICM/D	ICM	Direct	ICM/D
1.477	1.312	1.125	1.724	1.712	1.007	1.624	1.510	1.075
1.296	1.168	1.109	1.477	1.487	0.993	1.020	0.920	1.109
0.933	0.843	1.107	1.474	1.428	1.032	0.875	0.825	1.060
0.861	0.823	1.046	1.205	1.229	0.981	0.775	0.705	1.100
Starboard side average ICM/D = 1.013								

Table 3 Calculated ice pressures on the port side and the starboard side (2nd test). (unit : *MPa*)

L3			L6			L9		
ICM	Direct	ICM/D	ICM	Direct	ICM/D	ICM	Direct	ICM/D
1.852	1.804	1.026	1.668	1.560	1.069	2.836	2.632	1.078
1.191	1.201	0.992	1.306	1.330	0.982	1.110	1.168	0.951
1.184	1.085	1.092	1.192	1.178	1.012	1.191	1.080	1.103
1.020	1.074	0.950	0.891	0.938	0.950	1.075	1.048	1.026
Port side average ICM/D = 1.012								
R3						R9		
ICM	Direct	ICM/D				ICM	Direct	ICM/D
2.184	1.956	1.117				1.341	1.184	1.133
1.054	0.929	1.134				0.936	0.880	1.063
0.755	0.769	0.982				0.825	0.863	0.956
0.755	0.694	1.088				0.847	0.752	1.127
Starboard side average ICM/D = 1.067								

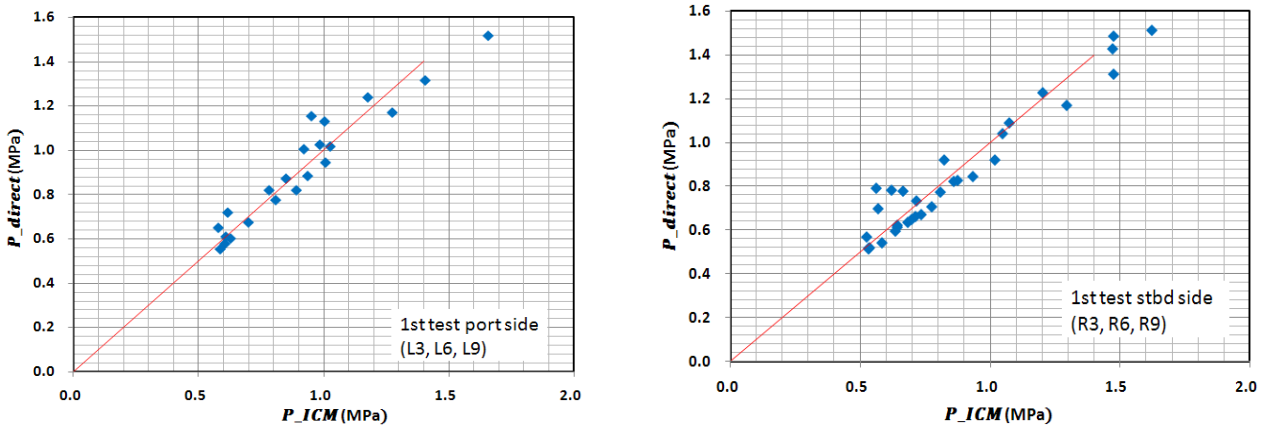

Fig. 10 Pressures obtained by ICM and direct method (1st test).

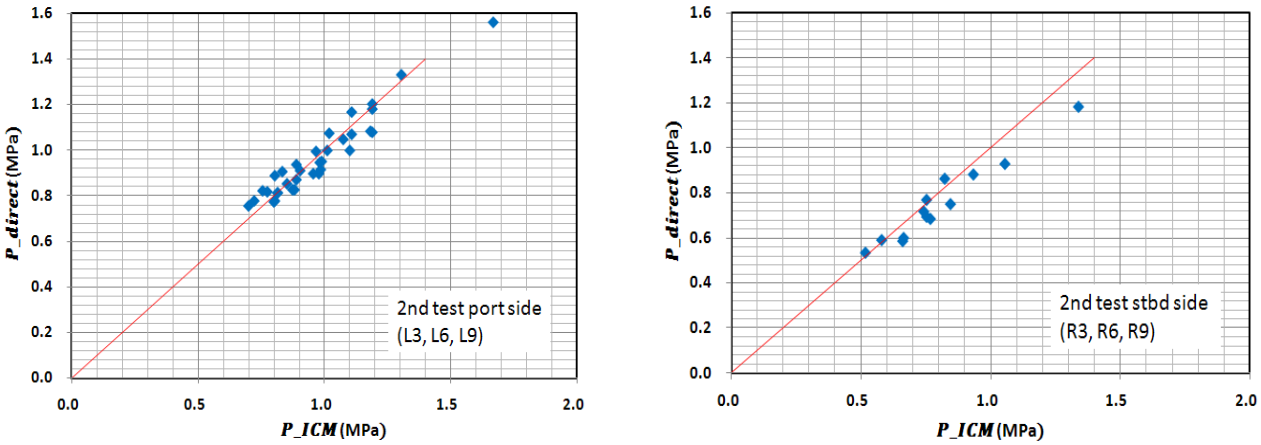

Fig. 11 Pressures obtained by ICM and direct method (2nd test).

Comparison of the ice load measured on the port & the starboard sides

The stress values during the ice breaking tests were measured simultaneously by attaching the strain gauges in the same position on the port and the starboard sides. Three largest values from each measurement sequence and the values measured on the opposite side measured in the same time zone were compared and shown in the Table 4. In the table, 'Time' refers to the duration after the initial measurement in each test. From Table 4, it can be seen that one side has a higher peak value than the other side. Namely, it was measured as 3.65 *MPa* at L2 of port side when the stress has a maximum value of 99.79 *MPa* at R2 of starboard side. The ratio for measurements of port and starboard sides was about 3.7%.

Table 4 Comparison of peak stresses at the port and the starboard sides.

Test No.	Port	Peak stress (*MPa*)	STBD	Peak stress (*MPa*)	Time (*sec*)
1	L2	3.654	R2	99.79	981.28
	L3	77.33	R3	3.008	1048.36
	L8	76.2	R8	2.84	1134.4
2	L7	129.5	R7	2.645	2823.8
	L9	104.9	R9	3.635	2824.12
	L10	180.7	R10	3.941	2823.76

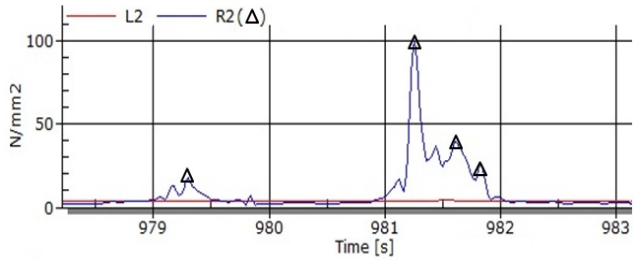

Fig. 12 Example of peak stress measured in the 1st test.

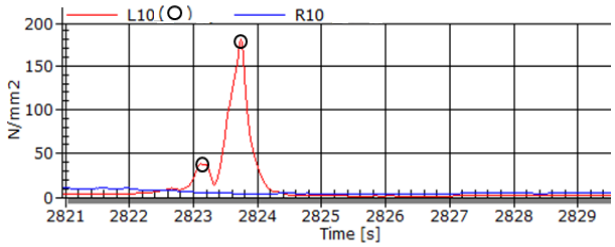

Fig. 13 Example of peak stress measured in the 2nd test.

The maximum and the average values of the stress ratio for peak stress over 20 *MPa* in Test 1 were 34.1% and 12.8%, whereas in Test 2, the values were 70.8% and 16.6%, respectively. For peak stress over 50.0 *MPa*, the maximum and the average stress ratio of both sides in the first test were 14.2% and 6.3%, whereas in the second test the corresponding values were 20.2% and 6.6%, respectively. These results showed that the measured values from both sides have a large difference, especially when comparatively large peak stress values were compared.

The stress values obtained for the port and the starboard sides during the ice breaking test in the same time zone are shown in Figs. 12 and 13. These values correspond to the time zone when the peak values were maximums in the first test. Fig. 11 shows that R2 of the starboard side had the maximum peak value in the first test, and L2 value of the port side showed a small change in the same time zone. This can be attributed to the difference in contact of the two sides with the ice floe during the ice breaking test.

Fig. 14 also shows the stress measured in the opposite sides at the same time in each time zone based on the peak stress over 20 *MPa* during the first ice breaking test. In order to distinguish the port side from the starboard side of the ship intuitively, the stress measured on the port side was treated as a negative number. There was almost no such case where the large stress could be measured on both the sides simultaneously. This clearly indicated that simultaneous contacts on both sides did not occur during the ice breaking tests and was considered unusual. The peak stress, in most of the cases occurs alternately on both the sides. During ice breaking, if the influence of sea waves is ignored, the change in the course of the ship can be simply assumed to be due to the resistance offered by the ice in contact with the vessel.

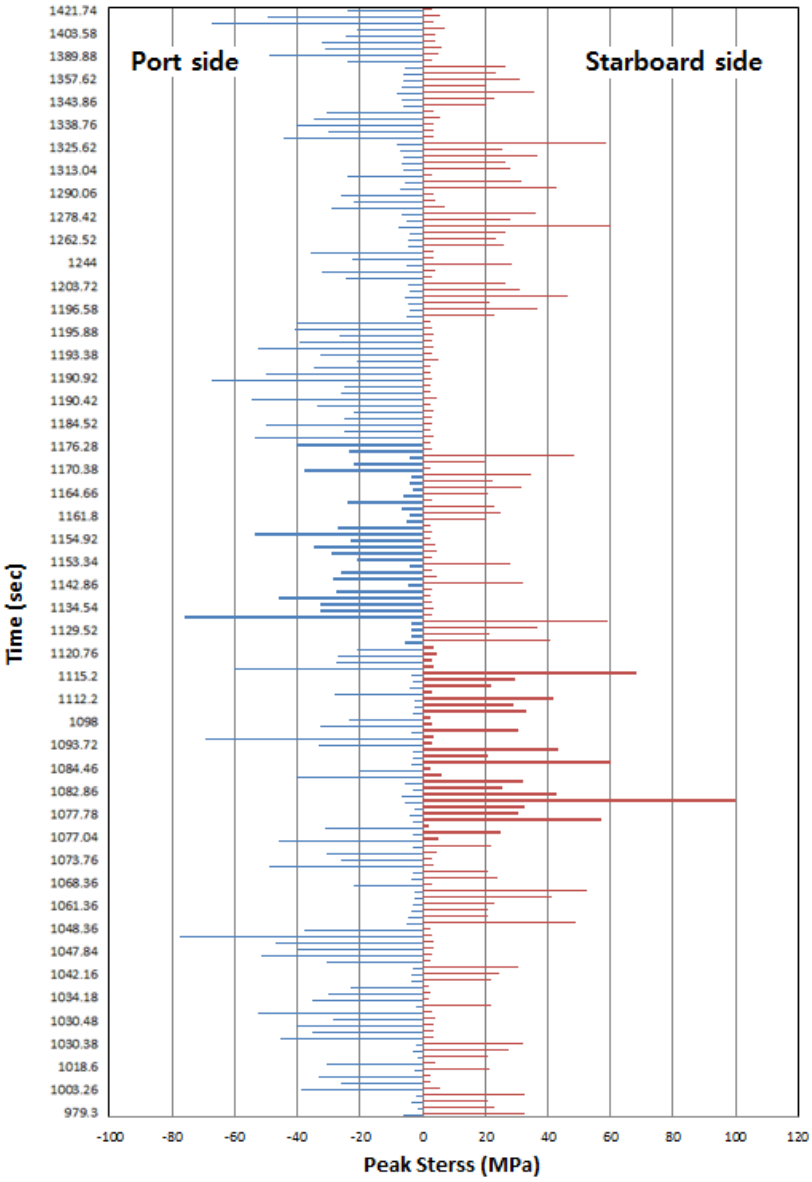

Fig. 14 Comparison of stresses at both the sides (1st test).

CONCLUSIONS

This study was conducted for the conversion of ice pressure using the strain data measured at Amundsen Sea near the Antarctic in 2012. The ice load which was applied to the bow of ship was measured by attaching the strain gauges inside the shell plating of port and starboard side.

Based on this, after the ice pressure was converted using the influence coefficient method and the direct method, the maximum value was 2.836 *MPa* when the influence coefficient method was used and 2.632 *MPa* when the direct method was used. As the average value of ICM/D ratio was close to 1, it can be said that there was almost no difference between the values. Therefore, the direct method can be used to calculate the ice pressure for engineering purpose.

The peak stresses measured at the symmetric points of the port and the starboard sides in each time zone were also compared. From the result, the measured ice load in the middle of the ice breaking test showed a large difference between the port and the starboard sides. From this, it can be concluded that the ice contact situations on the port and the starboard sides were not similar. Especially, when comparatively high level peak stress was measured, the relative ratio was below 7% in average.

ACKNOWLEDGEMENTS

This research was supported by BK21 Plus project. The authors gratefully acknowledge this support.

REFERENCES

ABS, 2011. *Guide for ice load monitoring system*. Houston, TX: ABS.

Choi, K.S., Kim, H.S., Choi, G.G., Lee, J.M. and Ha, J.S., 2012. *Voyage activity report : 2012 Amundsen Sea voyage of the icebreaking research vessel "ARAON"*. Daejeon: Ice Field Test and Research Team.

Ha, J.S., Choi, K.S., Kim, H.S., Choi, G.G. and Lee, J.M., 2012. Measurements for material properties of Sea Ice in the Amundsen Sea of the Antarctic and icebreaking performance tests of icebreaking research vessel ARAON. *Proceeding of the Society of the Naval Architects of Korea*, Daegu, 31 May - 1 June 2012, pp.546-549.

ISSC, 2012. Arctic technology committee V.6 report. *18th International Ship and Offshore Structures Congress*, Rostock, Germany, 09-13 September 2012, pp.243-274.

Kim, H.S., Lee, C.J., Choi, K.S. and Kim, M.C., 2011. Study on icebreaking performance of the Korea icebreaker ARAON in the arctic sea. *International of Journal of Naval Architecture and Ocean Engineering*, 3, pp.208-215.

Kim, H.S., Lee, C.J. and Choi, K.S., 2012. Speed trial analysis of Korean ice breaking research vessel 'Araon' on the big floes. *Journal of the Society of Naval Architects of Korea*, 49(6), pp.478-483.

Kim, H.S., Kim, M.C., Choi K.S. and Lee, C.J., 2013. Full scale ice sea trials of Korean ice breaking research vessel 'Araon' on the big floes near Antarctica. *Journal of Marine Science and Technology*, 18, pp.515-523.

Kim, T.W., Kim, H.N., Choi, K.S. and Lee, T.K., 2014. Study on influence of ship speed on local ice loads on bow of the IBRV ARAON. *Proceedings of the Twenty-fourth (2014) International Ocean and Polar Engineering Conference*, Busan, Korea, June 15-20 2014, pp.1159-1164.

Lee, T.K., Lee, J.H., Rim, C.W. and Choi, K.S., 2013a. Effects of ship speed and ice thickness on local ice loads measured in Arctic Sea. *Journal of Ocean Engineering and Technology*, 27(5), pp.82-87.

Lee, T.K., Kim, T.W., Rim, C.W. and Kim, S.C., 2013b. A study on calculation of local ice pressures for ARAON based on data measured at Arctic Sea. *Journal of Ocean Engineering and Technology*, 27(5), pp.88-92.

Park, Y.J., Kim, D.H. and Choi, K.S., 2011. Material properties of Arctic Sea ice during 2010 Arctic voyage of icebreaking research vessel ARAON: Part 1-Sea ice thickness, temperature, salinity and density. *Journal of Ocean Engineering and Technology*, 25(2), pp.55-61.

Ritch, R., Frederking, R., Johnston, M., Browne, R and Ralph, F. 2008. Local ice pressures measured on a strain gauge panel during the CCGS Terry Fox bergy bit impact study. *Cold Regions Science and Technology*, 52(1), pp.29-49.

St. John, J.W., Daley, C. and Blount, H., 1990. *Ice loads and ship response to ice -summer 1982/winter 1983 test program-, Ship Structure Committee (SSC), report no. 329*, Washington: SSC.

St. John, J.W. and Minnick, P.V., 1995. *Ice load impact study on the national science foundation's research vessel Nathaniel B. Palmer. Ship Structure Committee (SSC), report no. 376*, Washington: SSC.

Timco, G.W. and O'Brien, S., 1994. Flexural strength equation for sea ice. *Cold Regions Science and Technology*, 22(3), pp.285-298.

Tsoy, L.G., Karavanov, S.B., Glebko, Y.V., Barabanov, N.V., Babich, N.G., Karlov, V.K. and Shatsberger, E.M., 1998. *Collection of SA-15 operations data. INSROP(International Northern Sea Route Programme) working paper no. 107*. St. Petersburg: INSROP.